Modeling Habituation with Neural Mass Model

Peng Wang & Thomas R. Knösche

Max Planck Institute for Human Cognitive and Brain Sciences, Leipzig, Germany
pengwang@cbs.mpg.de

MAX PLANCK INSTITUTE | FOR HUMAN COGNITIVE AND BRAIN SCIENCES LEIPZIG

Introduction

The short term habituation (STH) effect is observed in event-related electroencephalographic (EEG) and magnetoencephalographic (MEG) data of auditory experiments. More specifically, the N100 component of the evoked potential/field decreases from stimulus to stimulus when presenting trains of identical stimuli [1]. To investigate and mimic the underlying mechanism of this phenomenon, we extend the biologically plausible neural mass model (NMM), which first presented by Jansen and Rit [2], with an additional differential equation, which describes the STH as a function of the repetition of the stimuli. The model parameters are estimated from MEG data using a Bayesian inference scheme [3].

Methods

Stimulation

A healthy human volunteer was stimulated by earphones with 160 trains of ten identical tones (900Hz, 15ms) each. The tones were separated by 500ms and the trains were separated by 10s. The subject was watching a silent movie during recording.
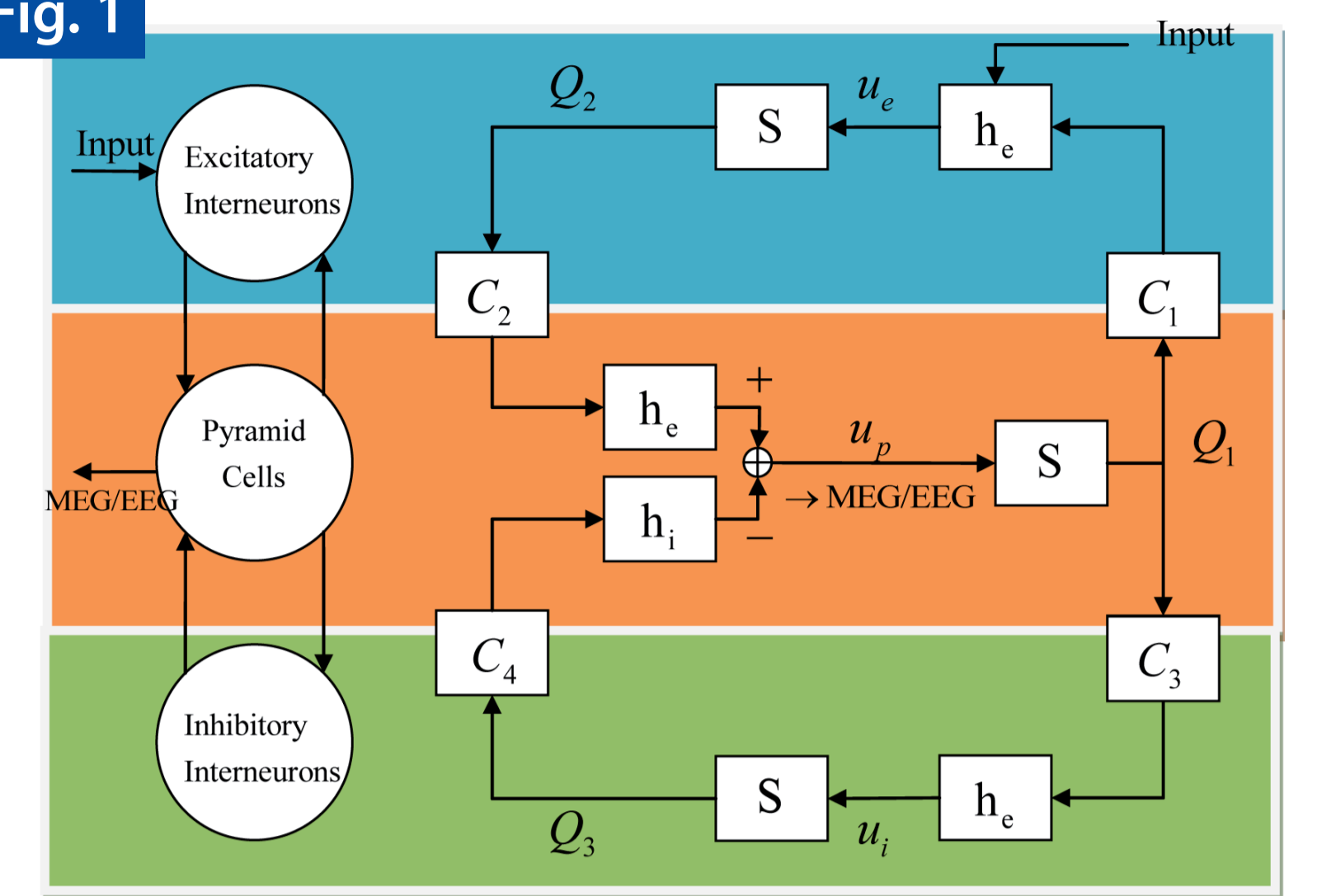
Data

MEG data were recorded by 306 channels (204 gradiometers and 102 magnetometers) around the whole head at a sampling rate of 1000Hz. Only the channels on the right side of the hemisphere (102 gradiometers and 51 magnetometers) were used for the equivalent current dipole estimation and the model parameter estimation. The data were averaged over trains offline (time window: -100ms to 2500ms, including five stimuli, first stimulus at the time point 0). A band pass filter (1 Hz to 20 Hz) was applied to reduce the noise.

Model

Neural mass model for a single cortical column

According to the model of Jansen and Rit [2], a cortical area can be considered as three interacting neuronal populations: pyramidal cells, excitatory interneurons and inhibitory interneurons. Two key operators describe the behavior of the neuronal populations. The first one transforms the average density of pre-synaptic spikes arriving at the population into the average postsynaptic membrane potential (PSP). The second operator transforms the average membrane potential of the population into the average pulse density of action potentials fired by the neuron (figure 1).

Model of auditory evoked field

The model of auditory evoked field (AEF) is constructed by using two NMMs (figure 2). This structure is based on the notion that there are (at least) two separated auditory cortex sources that contribute for the N100 component: an early one at about 85ms, which associates with the sound feature "where" and a late one at about 150ms, which associates with the sound feature "what" [4]. In order to link the model to the MEG a lead field matrix (LFM) is necessary. For each NMM an equivalent current dipole (at 80ms for "where" and at 135ms for "what") was used to localize the anatomical source position for the LFM calculation.

Model of STH

We expect that the decrease of the N100 amplitude can be explained by reduction of the excitatory intrinsic connectivity between the neuronal populations (pyramid cells to excitatory/inhibitory interneurons, excitatory interneurons to pyramid cells) [5] and this assumption is implemented as a differential equation:

$$\begin{cases} \dot{W} = -n_1 W \dfrac{Q}{Q_{max}} + n_2(1-W), & (Q \geq 0) \\ \dot{W} = n_2(1-W), & (Q < 0) \end{cases}$$

where W $(0 \leq W \leq 1)$ is the weight that scales the synaptic connection efficiency between two intrinsic neuronal populations. Q is the pre-synaptic firing rate. Q_{max} denotes the maximally possible firing rate. n_1 and n_2 govern the habituation rate and the recovery rate. The first term describes that the connectivity will reduce as a function of the current connectivity and incoming pre-synaptic activity, i.e. the pre-synaptic firing rate in our model and the second term describes the recovery of the connectivity.

Fig. 1

$$h(t) = \begin{cases} \dfrac{H_{e,i}}{\tau_{e,i}} t e^{-\frac{t}{\tau_{e,i}}} & t \geq 0 \\ 0 & t \leq 0 \end{cases}$$

h: rate-to-potential operator

$$Q(u) = \frac{2e_0}{1-\exp(r(u_0-u))} - \frac{2e_0}{1-\exp(ru_0)}$$

S: potential-to-rate operator

$$P(t) = q(\frac{w}{t})^n e^{-\frac{w}{t}}$$

Input:

Figure 1. General structure of a cortical area. Three neuronal populations are considered to model a cortical area. is the rate-to-potential operator. is the potential-to-rate operator. are the connectivity among the populations (more details for the model parameters see [1]). The EEG/MEG signal is proportional to the PSP of the pyramid cells.
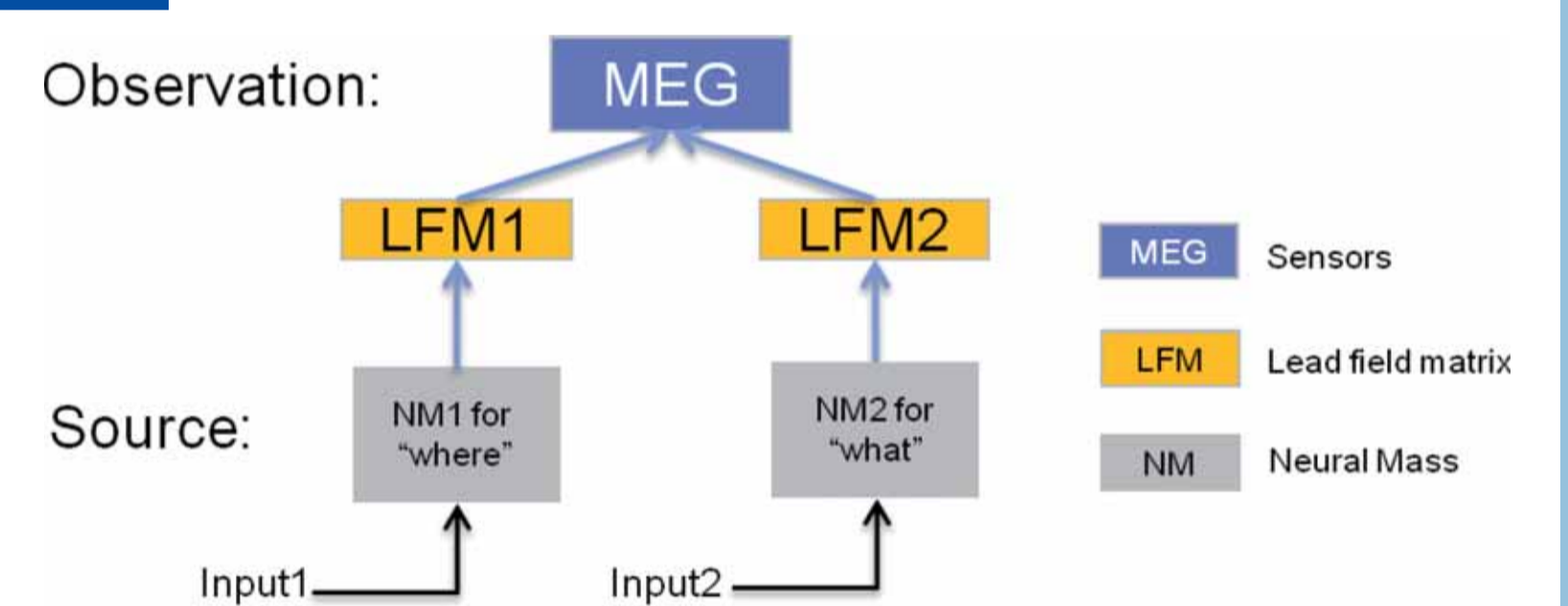

Fig. 2

Figure 2. Architecture of the model of the auditory evoked field. There are two sources contribute the N100 component. An early activated source associates with the sound feature "where". A late activated source associates with the sound feature "what". The measured MEG is assumed to be equal to the source output multiplied with the lead field matrix.

Results

Following the Bayesian inversion scheme in [3] we estimated 18 parameters to fit the AEF. These were: $\tau_e, \tau_i, C_1, C_2, C_3, C_4$ for each neural mass (for more details about the parameters see [1]); the input time duration w for both inputs P_1 and P_2 (We simply assumed that the inputs of the two NMMs were same.) ; the constant time delay d between input P_1 and P_2 ; the habituation rate n_1 and n_2 the recovery rate for each neural mass. We used the same habituation rate and the recovery rate for all three excitatory intrinsic connections inside a neural mass. In figure 3 we present the observed AEFs in yellow and the simulated AEFs in blue. We fitted the parameter using the data set with three stimuli and predicted the fourth and fifth evoked fields.

Fig. 3

N100

−100 ms   1500 ms

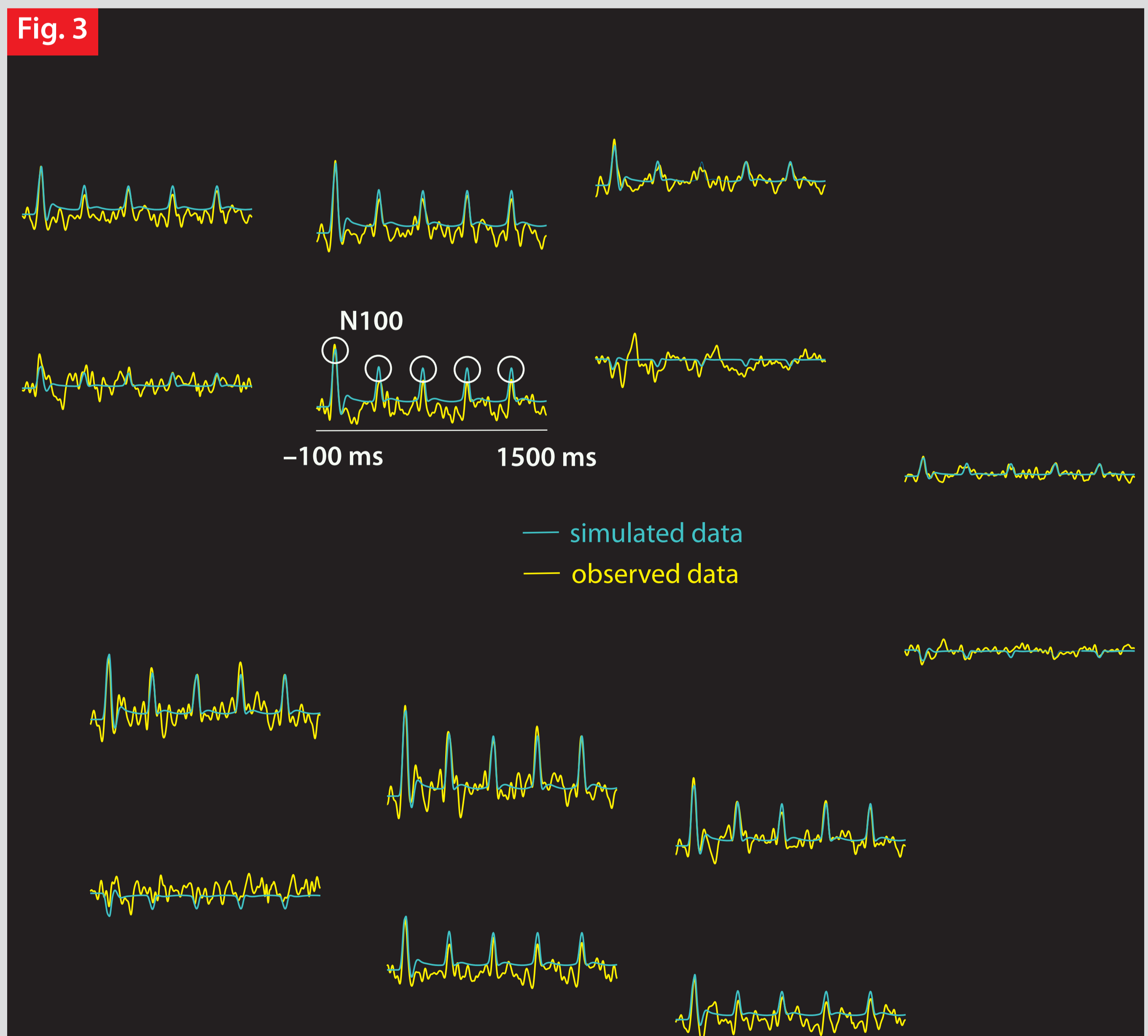— simulated data
— observed data

Figure 3. Observed and simulated auditory evoked fields near the right temporal lobe (recorded by 14 gradiometers). We fitted the model parameters using the observed MEG with the first three stimuli and predicted the fourth and the fifth responses of the stimuli.

Discussion & Conclusion

We attempted to model the plasticity of the connectivity between the neural populations as the function of the stimulus repetition. The N100 is sensitive to the STH. With our habituation model we were able to fit the auditory N100 component and its decreasing amplitude during receptive stimulation. With this simplified model, which we focused only on the dynamic of the N100 component and we did not attempt to fit earlier components such as P50 and later components such as P200, P300 etc. In order to keep the balance between the model complexity and the fitting we chose only two columns to model the whole AEF, which omits a lot of signal details. Of course, one could use a more detailed model that includes more sources, but then we would also need more data. Here, we provide proof of principle that the suggested mechanism is capable of predicting the habituation effect.

The feature of the classical neuronal mass model is that it links the EEG/MEG with physiological parameters. Extending the model with a subsystem, which describe the slow change of the parameters, can simulate learning process such as habituation. Combining forward modeling and the Bayesian inverse method could be useful to investigate physiological parameters and the underlying neuronal mechanisms.

Reference

1. Rosburg, T., et al., *Habituation of auditory evoked potentials in intracranial and extracranial recordings.* Psychophysiology, 2006. **43**(2): p. 137-44.
2. Jansen, B. and V. Rit, *Electroencephalogram and visual evoked potential generation in a mathematical model of coupled cortical columns.* Biological Cybernetics, 1995. **73**(4): p. 357-366.
3. Friston, K., et al., *Classical and Bayesian inference in neuroimaging: applications.* Neuroimage, 2002. **16**(2): p. 484-512.
4. Ahveninen, J., et al., *Task-modulated "what" and "where" pathways in human auditory cortex.* Proceedings of the National Academy of Sciences, 2006. **103**(39): p. 14608.
5. Glanzman, D.L., *Habituation in Aplysia: the cheshire cat of neurobiology.* Neurobiology of learning and memory, 2009. **92**(2): p. 147-154.